Multiple distinct evolutionary mechanisms govern the dynamics of selfish mitochondrial genomes

Bryan L. Gitschlag[1,2]*, Claudia V. Pereira[1,#], James P. Held[1], David M. McCandlish[2], & Maulik R. Patel[1,3,4,5]*

[1]Department of Biological Sciences, Vanderbilt University, Nashville, TN, USA

[2]Simons Center for Quantitative Biology, Cold Spring Harbor Laboratory, Cold Spring Harbor, NY 11724

[3]Department of Cell and Developmental Biology, Vanderbilt University School of Medicine, Nashville, TN, USA

[4]Diabetes Research and Training Center, Vanderbilt University School of Medicine, Nashville, TN, USA

[5]Evolutionary Studies, Vanderbilt University, VU Box #34-1634, Nashville, TN, USA

[#]Present address: Nvelop Therapeutics, Cambridge, MA, USA

**Corresponding authors*: gitschl@cshl.edu (BLG); maulik.r.patel@vanderbilt.edu (MRP)

ABSTRACT

Cells possess multiple mitochondrial DNA (mtDNA) copies, which undergo semi-autonomous replication and stochastic inheritance. This enables mutant mtDNA variants to arise and selfishly compete with cooperative (wildtype) mtDNA. Selfish mitochondrial genomes are subject to selection at different levels: they compete against wildtype mtDNA directly within hosts and indirectly through organismal selection. However, determining the relative contributions of selection at different levels has proven challenging. We overcome this challenge by combining mathematical modeling with experiments designed to isolate the levels of selection. Applying this approach to many selfish mitochondrial genotypes in *Caenorhabditis elegans* revealed an unexpected diversity of evolutionary mechanisms. Some mutant genomes persist at high frequency for many generations, despite a host fitness cost, by aggressively outcompeting cooperative genomes within hosts. Conversely, some mutant genomes persist by evading organismal selection. Strikingly, the mutant genomes vary dramatically in their susceptibility to neutral drift. Although different mechanisms can cause high frequency of selfish mtDNA, we show how they give rise to characteristically different distributions of mutant frequency among individuals. Given that heteroplasmic frequency represents a key

determinant of phenotypic severity, this work outlines an evolutionary theoretic framework for predicting the distribution of phenotypic consequences among individuals carrying a selfish mitochondrial genome.

INTRODUCTION

Major evolutionary transitions follow a similar adaptive logic from solitary to social living as from unicellular to multicellular life, prokaryotic to eukaryotic cells, and molecular replicators to cells and genomes.[1-3] In each case, previously independent entities form a cooperative group that reproduces and undergoes natural selection as a unified collective.[1-5] By contributing to the fitness of other group members, however, cooperative interactions can select for selfish, "cheater" entities,[6-9] which occur at each level of biological organization, from the molecular to societal.[9-13] Although cheating confers an advantage within groups, by assuming the benefits without the costs of cooperation,[6] cheaters also face disadvantages for numerous reasons. These include suppression or "policing" mechanisms that enforce cooperation, as well as negative frequency-dependent selection, that is, declining fitness as cheaters become more frequent.[12,14] Selection at higher levels of biological organization, which rely on cooperation, can also counter the fitness advantage of cheaters, consistent with observations ranging from selfish genetic elements to animal societies.[10,14-17] Thus, different evolutionary mechanisms, such as multilevel and frequency-dependent selection, are thought to help resolve an apparent paradox, namely the coexistence of cooperative and selfish entities.[12,14-17]

Like other major evolutionary transitions, the origin of the eukaryotic cell led to conflicting strategies of cooperation and cheating. This arises from the fact that mitochondria retain their own DNA (mtDNA), a remnant of their bacterial ancestor, whose symbiotic relationship with the nucleus serves as both the foundation of eukaryotic life and as a source of genetic conflicts.[18-20] In contrast to the typically diploid nuclear genome, an animal cell contains hundreds or thousands of mtDNA molecules,[21,22] which replicate asynchronously throughout the cell cycle.[23,24] High mtDNA copy number and relaxed, semi-autonomous replication frequently give rise to a heteroplasmic state, in which a host organism harbors a mixed

51 population of different mtDNA variants. Competition for replication and transmission can select for
52 mutations that confer a selfish advantage over other mtDNA variants within a host, whereas host fitness
53 constitutes a form of group selection favoring cooperative genomes.[18,25-28] Mitochondria thus serve as an
54 exceptional case study for understanding the dynamics of cooperation and conflict.
55
56 Consistent with the conceptual framework of multilevel selection, prior research has uncovered numerous
57 insights into the molecular, physiological, and environmental determinants of the fitness effects of
58 mitochondrial mutations.[29-32] Many such findings can be credited to the mutant genome *uaDf5* in the model
59 species *Caenorhabditis elegans*.[26,30-39] Due to a 3.1-kilobase deletion resulting in the loss of four protein-
60 coding and seven tRNA genes (Fig. 1a), *uaDf5* negatively impacts mitochondrial respiration and host
61 fitness.[26,34-36] Despite these effects, *uaDf5* can persist alongside cooperative (wildtype) mtDNA in a
62 heteroplasmic state for hundreds of generations.[38] How is this accomplished? In agreement with theory,[40]
63 experimental work has shown that *uaDf5* propagates not only in spite of but *because* of its adverse effects,
64 by exploiting physiological stress-resistance mechanisms,[32,34,36] consistent with *uaDf5* being a bona fide
65 cheater.[6] On one hand, these findings highlight *uaDf5* as a valuable model of a biological cheater. On the other
66 hand, a disproportionate fraction of mechanistic insights have come through studying this
67 genome,[18,26,27,29,30,32,34,36,37,39] which challenges the ability to draw broad conclusions. Moreover, although
68 prior studies have implicated diverse mito-nuclear interactions in the selfish propagation of mitochondrial
69 mutations,[26,29,32,34,36,41] as well as substantial variation in their phenotypic effects,[42,43] this work spans
70 multiple species.[18,27,29] Because animal species vary widely in ways that affect mitochondrial genome biology,
71 including nuclear genome composition, development and organization of the germline, and environmental
72 context,[29,44] these numerous confounding factors have strongly limited our ability to draw general
73 conclusions about the evolutionary dynamics of selfish mitochondrial genomes.
74

75 To address these challenges, we developed an approach that leverages a collection of mutant mitochondrial
76 genotypes within a single species, namely *C. elegans*. In particular, we combine mathematical modeling with
77 laboratory experiments to comprehensively measure the evolutionary forces that govern the population
78 dynamics of these stable heteroplasmies. First, we introduce a stochastic population genetic model of selfish
79 mitochondrial genomes, which includes different levels of selection (organismal and intra-organismal) plus
80 genetic drift. Theoretical modeling revealed that different evolutionary mechanisms give rise to qualitatively
81 similar outcomes, such as the persistence of a mutant genome at high heteroplasmic frequencies. Despite
82 these qualitative similarities, however, the distribution of mutant frequencies among hosts contains
83 information about the underlying evolutionary forces. To test our theoretical results, we fit our model to
84 empirical data, obtained from experiments designed to disentangle the levels of selection. We applied this
85 approach to a collection of mitochondrial genotypes, encompassing mutations that affect enzyme complexes
86 I, III, and IV of the electron transport chain (ETC), in addition to the well-known mutant mtDNA variant *uaDf5*
87 (Fig. 1a). Importantly, although each mutant genome stably propagates in heteroplasmic lineages, the
88 distribution of mutant frequencies among heteroplasmic individuals varies considerably between these
89 genotypes (Fig. 1b). Indeed, consistent with our theoretical analysis, we find that although cheating is a
90 common feature of mutant mitochondrial genomes, the evolutionary mechanisms comprising their cheating
91 "strategy," and which maintain these observed distributions of mutant frequencies, are fundamentally
92 different depending on the affected loci.
93
94 **RESULTS**
95 **Population genetic modeling implicates multiple mechanisms in the dynamics of selfish**
96 **mitochondrial genomes**
97 To understand the complex population genetics of selfish mitochondrial genomes, we developed a
98 population-genetic model that captures natural selection at the organismal and intra-organismal levels, as

well as genetic drift within heteroplasmic lineages in order to reflect stochasticity in development and mitochondrial inheritance.

For selfish mtDNA mutants, let us first consider how mutant mtDNA frequency within an individual, z, changes between parent and progeny (Fig. 1c, top row). To capture this effect, we define the intra-organismal fitness function $w_{intra}(z)$ to be the net relative replication success of selfish versus cooperative (wildtype) mtDNA, per organismal generation, as a function of z. Thus, mutant frequency tends to increase when $w_{intra}(z)>1$ but tends to decrease when $w_{intra}(z)<1$. We use a three-parameter fitness function, which can accommodate frequency-dependent or frequency-independent fitness effects and either linear or nonlinear frequency-fitness relationships (see Methods for details). While the intra-organismal fitness function and current mutant mtDNA frequency z determine the expected mutant mtDNA frequency among progeny, to capture stochasticity during development and inheritance, we model these dynamics phenomenologically as consisting of a single generation of a Wright-Fisher process where in each generation mtDNA passes through a developmental bottleneck of size N. In our modeling framework N is best viewed as an effective or "virtual" mtDNA bottleneck size, since it reflects the cumulative effect of drift throughout the organismal lifecycle, both during early development and in the adult germline.

Moving to the organismal level, we treat the inter-organismal dynamics deterministically, corresponding to the case of an infinite population of heteroplasmic hosts. We define organismal fitness $w_{org}(z)$ as the expected number of viable offspring per heteroplasmic parent with mutant mtDNA frequency z, divided by the expected number of viable offspring per homoplasmic-wildtype parent. We assume a model of purifying selection, so that organismal fitness is monotonically decreasing with increasing selfish mtDNA frequency (Fig. 1c, bottom row), with organisms fixed for the mutant mtDNA becoming sterile or inviable (that is, $w_{org}(1)=0$), since the mutations investigated here delete one or more essential respiratory gene(s). Because previous heteroplasmy studies have observed threshold effects, whereby modest shifts in mutant frequency

124 can have large phenotypic consequences,[45,46] we fit a two-parameter fitness function that can accommodate
125 both simple linear and power-law models for how the organismal fitness cost scales with selfish mtDNA
126 frequency, as well as more complicated threshold-like models (see Methods for details).
127
128 Combining our organismal and intra-organismal models, each generation begins with a distribution of
129 mutant mtDNA frequencies among heteroplasmic hosts. These frequencies are shifted by intra-organismal
130 selection and the distribution is broadened by intra-organismal drift. Finally, host organisms reproduce with
131 an expected number of viable offspring determined by their mutant mtDNA frequency. As this process
132 repeats across generations, the distribution of mutant mtDNA frequencies among hosts approaches a
133 characteristic shape (given by the dominant eigenvector of a principal submatrix of the transition matrix
134 describing the above evolution process, see Methods), where the shape of this stable mutant frequency
135 distribution reflects the specific parameter values employed. From this distribution, we can calculate the
136 mean fitness of heteroplasmic carriers relative to their wildtype counterparts, as well as the rate of
137 spontaneous reversion to the homoplasmic-wildtype state due to the *de novo* loss of the mutant genome via
138 intra-organismal drift. Together, these values determine the timescale over which an established
139 heteroplasmy will be lost, which can either be short or long depending on the specific parameters. Indeed,
140 under this model we observe that selfish mtDNA can persist in a heteroplasmic state for hundreds, or even
141 thousands, of generations under biologically realistic population genetic conditions.
142
143 Examining this model led us to identify a number of distinct evolutionary mechanisms that determine the
144 stable distribution of mutant mtDNA frequencies (Fig. 2). Under the first mechanism, intra-organismal
145 balancing selection, the intra-organismal fitness advantage of the mutant genome vanishes in favor of the
146 wildtype genome at a frequency z^* that is still too low to encounter significant organismal selection (Fig.
147 2a,b); that is, there exists a frequency z^* with $w_{intra}(z^*)=1$ and $w_{org}(z^*)\approx 1$. The mutant frequency distribution

among hosts is therefore centered at approximately z^* and is subject to negligible organismal selection, with genetic drift determining the width of the distribution (Fig. 2c).

Under the second mechanism, which could be termed strong multilevel selection, a mutant genome maintains an intra-organismal fitness advantage across all heteroplasmic frequencies, so that there exists no frequency z^* such that $w_{intra}(z^*)=1$ (Fig 2d). Thus, intra-organismal selection constitutively mutant frequency up into a range that elicits a strong organismal fitness cost (Fig. 2e). Under this mechanism, the stable mutant mtDNA frequency distribution is determined predominantly by the forms of the opposing organismal and intra-organismal selection, and is relatively insensitive to changes in the strength of intra-organismal drift, particularly for large mtDNA effective bottlenecks N (Fig. 2f).

Finally, in the third mechanism, there exists an intra-organismal equilibrium frequency z^* with $w_{intra}(z^*)=1$, but the organismal fitness cost intensifies rapidly at frequencies similar to z^* (Fig. 2g,h). Under this mechanism, the shape of the distribution depends on the form of all three forces, namely intra-organismal selection, organismal selection, and drift (Fig. 2i). We therefore call this the mixed mechanism. Together, these findings suggest that mitochondrial mutations can persist at similar heteroplasmic frequencies despite substantial differences in the underlying evolutionary mechanisms. Understanding the mechanisms relevant to any given selfish mitochondrial genome therefore requires that our model be integrated with experiments to measure both selection and drift within hosts, in addition to organismal selection.

Integrating theory with experiment reveals the evolutionary mechanisms of a selfish mitochondrial genome

As a first application of approach, we inferred the mechanisms determining the form of the stable mtDNA frequency distribution for the well-characterized selfish mitochondrial genome *uaDf5*. To measure intra-organismal selection in the absence of organismal competition, we tracked mutant frequency longitudinally,

173 between isolated individual parents and their respective age-matched progeny (Fig. 3a, see Methods).[26] At
174 the organismal level, fitness is expected to depend on heteroplasmic frequency, which itself is in flux over
175 the course of organismal development due to intra-organismal selection and drift. This greatly limits our
176 ability to assess the organismal component of selection directly by comparing the fitness of different
177 heteroplasmic hosts. To overcome this challenge and estimate the organismal fitness effects of selfish
178 mtDNA, we instead competed a diverse cohort of heteroplasmic animals against their homoplasmic-wildtype
179 counterparts on the same food plate (Fig. 3b). Since the heteroplasmic cohort is taken from a stock
180 population stably maintaining the selfish mtDNA, the strength of selection against the heteroplasmy reflects
181 the overall fitness of this stable frequency distribution relative to a population lacking the selfish genome, as
182 well as the rate of *de novo* loss of heteroplasmy by genetic drift. Finally, we also collected information on the
183 shape of the stable mutant mtDNA frequency distribution by measuring *uaDf5* frequency in multiple fertile
184 adults sampled from a heteroplasmic stock population (Fig. 3c).
185
186 Using the above data (Fig. 3a-c), we inferred the parameters describing organismal fitness, intra-organismal
187 fitness and drift by maximum likelihood, employing a parametric bootstrap procedure to assess uncertainty
188 (Fig. 3d-f, maximum likelihood results in black, bootstrap replicates in red; see Methods for details;
189 Supplemental Fig. 1-3 confirm that our computational procedure can recover the true parameter for
190 simulated data). For *uaDf5*, we found strong evidence for negative frequency-dependent intra-organismal
191 selection (Fig. 3d), where the mutant genome has an intra-organismal advantage when present at low
192 heteroplasmic frequency ($w_{intra}(0)$=1.37, 95% bootstrap confidence interval 1.27–2.22), and fitness
193 decreases with frequency so that it likely faces an intra-organismal disadvantage at high frequency
194 ($w_{intra}(1)$=0.34, 95% bootstrap confidence interval $5.8*10^{-4}$–1.1; $w_{intra}(0)>w_{intra}(1)$ for 100% of bootstraps;
195 $w_{intra}(1)<1$ for 87% of bootstrap samples). Although our measure of intra-organismal drift is intended to be
196 phenomenological, our maximum likelihood estimate of N=29 (Fig. 3d inset, 95% bootstrap confidence
197 interval 20–100) is consistent with previous reports of the estimated effective mtDNA bottleneck in the

198 developing germline.[47] For organismal selection (Fig. 3d), we infer a threshold-like response, with essentially
199 no fitness cost at low heteroplasmic frequency ($w_{org}(z)$>0.99 for all z<0.5 in 92% of bootstrap samples), with
200 the sudden onset of a substantial fitness cost once the mutant reaches sufficiently high frequency
201 (organismal fitness is decreased by half, $w_{org}(z)$=0.5, at z=0.77, 95% bootstrap confidence interval 0.75–
202 0.82). Together, these parameters predict a strongly left-skewed stable mutant mtDNA frequency
203 distribution among hosts (Fig. 3f), as observed in the data (Fig. 3c), a moderate growth defect for the
204 heteroplasmic relative to the wildtype sub-population (relative growth rate of 0.77, 95% bootstrap
205 confidence interval 0.75–0.80), and a low rate of *de novo* loss of heteroplasmy (per-generation probability of
206 mutant loss of $4.1*10^{-4}$, 95% bootstrap confidence interval $3.7*10^{-6}$–$1.1*10^{-3}$). Finally, variation in N is
207 predicted to substantially impact both the spread and location of the stable *uaDf5* frequency distribution
208 (Supplementary Fig. 4a-c), consistent with the mixed-mechanism hypothesis (Fig. 2g-i). These results
209 suggest that intra-organismal selection, organismal selection, and genetic drift are all important in the
210 dynamics of *uaDf5*.
211
212 **Diverse evolutionary mechanisms in the dynamics of selfish mitochondrial genotypes**
213 We sought to compare our results for *uaDf5* with a larger panel of selfish mitochondrial genotypes that
214 exhibit a greater diversity of stable mutant frequency distributions (Fig. 1a,b). These include mutations
215 affecting ETC complex I (*mpt2*), complex III (*mptDf3*), and complex IV (*mptDf2* and *mpt4*), as well as affecting
216 tRNA genes (*mptDf2* and *mptDf3*). We measured selection and collected mutant frequency distribution data
217 (Fig. 4), using the same experimental approach used for *uaDf5*, and applied our theoretical analysis to these
218 data.
219
220 Overall, we find a surprising diversity of evolutionary mechanisms at play across this panel (Fig. 5),
221 representing all three of the distinct mechanisms described in Fig. 2. For example, although *mptDf2* and *mpt4*
222 have qualitatively similar stable mutant frequency distributions (Fig. 1b), *mptDf2* is governed by the mixed

223 mechanism, similar to *uaDf5*, whereas the distribution for *mpt4* is determined by strong multilevel selection,
224 with little influence of drift. The difference can be seen in Fig. 5a versus Fig 5d, where frequency-dependent
225 intra-organismal selection on *mptDf2* exhibits an internal equilibrium above which selection favors the
226 wildtype (maximum likelihood z^*=0.86, 95% bootstrap confidence interval 0.83–0.93) whereas *mpt4* is
227 constitutively favored by intra-organismal selection under the maximum likelihood fit ($w_{intra}(z)$>1 for all z
228 for 86% of bootstrap samples, z^* is greater than any empirically observed z in Fig. 4f for 98% of bootstrap
229 samples, and the few bootstrap replicates exhibiting z^*<1 have $w_{org}(z^*)$<0.2). Concordant with this analysis
230 of evolutionary mechanisms, we find that the stable *mptDf2* frequency distribution is sensitive to changes in
231 the mtDNA bottleneck size for (Supplementary Fig. 4f, compare Fig. 2i) whereas the stable *mpt4* frequency
232 distribution is relatively insensitive (Supplementary Fig. 4i, compare Fig. 2f). In contrast, we find that *mpt2*
233 persists primarily through intra-organismal balancing selection (Fig. 5g-i), with a stable mutant frequency
234 distribution centered on z^* (z^*=0.68, 95% bootstrap confidence interval 0.62–0.84), where *mpt2* frequency
235 is too low to experience substantial organismal selection ($w_{org}(z^*)$>0.99 for maximum-likelihood estimate
236 and $w_{org}(z^*)$>0.92 for 95% of bootstrap samples). Although *mpt2* results are consistent with a negligible role
237 for drift (Fig. 5g and Table 1, 95% bootstrap confidence upper limit of N=1,000), we also find evidence of
238 only weak selection at most (Fig. 5h and Table 1, relative growth rate >0.99 for maximum-likelihood estimate
239 and >0.91 for 95% of bootstrap samples). Furthermore, our analysis of the effects of changing the effective
240 mtDNA bottleneck N suggests that the width of the stable *mpt2* frequency distribution is highly sensitive to
241 genetic drift (Supplementary Fig. 4l, compare to Fig. 2c). Our modeling results for *mptDf3* are more
242 ambiguous (Fig. 5j-l and Table 1), due to uncertainty in the strength of organismal selection. Like *mpt2* but
243 in contrast to the other genotypes, average *mptDf3* frequency is not significantly different from z^*
244 (Supplementary Table 7), consistent with intra-organismal balancing selection. Finally, we find no significant
245 organismal selection against *mptDf3* (Fig. 4k and Table 1, relative growth rate 95% bootstrap confidence
246 upper limit >0.99), consistent with the maintenance of *mptDf3* via intra-organismal dynamics. We conclude

247 that although different evolutionary mechanisms maintain the heteroplasmic state, they also give rise to
248 idiosyncratic mutant frequency distributions.
249
250 Finally, we sought to explore the potential for long-term maintenance of the heteroplasmic state. We
251 reasoned that high heteroplasmic frequency and a strong intra-organismal advantage (in the case of *uaDf5*,
252 *mptDf2*, and *mpt4*) limits the probability of *de novo* mutant loss in finite populations, while a minimal
253 organismal cost (in the case of *mpt2* and *mptDf3*) limits the probability of successful invasion by a *de novo*
254 homoplasmic lineage. Using the inferred per-generation probability of mutant loss due to drift (Table 1),
255 together with the organismal fitness benefit of homoplasmic-wildtype state and previously published
256 theory,[48] we calculated likely persistence times of the heteroplasmic state, defined as the number of
257 generations until the probability of successful invasion is >0.5, for various values of effective organism
258 population size N_e. Prior estimates of N_e typically range from 200 to 10^4 for wild populations of *C. elegans*,[49]
259 whereas maintenance of laboratory strains involves the frequent transfer of small founding populations to
260 fresh food plates, resulting in an approximate per-generation bottleneck on the order of tens or hundreds of
261 *C. elegans*.[50] Modeling similar variation in N_e, we estimate a wide range of persistence times, reflecting joint
262 uncertainties in organismal fitness and probability of loss (Table 1). Unsurprisingly, our estimates are most
263 consistent with long-term persistence of the heteroplasmic state in small to mid-size populations
264 (Supplementary Table 6). With an N_e of 1,000, for example, our *uaDf5* data are consistent with a median time
265 till invasion on the order of hundreds of generations (95% bootstrap confidence upper limit of 342
266 generations). Likewise, our results for *mptDf2*, *mpt4*, and *mpt2* are consistent with a median time till invasion
267 on the order of 10^{22}, 10^{17}, and 10^9 generations (95% bootstrap confidence upper limits), respectively. For
268 even smaller populations with an N_e of 100, the data for *mptDf3* are likewise consistent with a median time
269 till invasion on the order of hundreds of generations (95% bootstrap confidence upper limit of 393
270 generations). We conclude that conditions influencing organism population size on one hand, and conflicting

271 selection pressures on the other, jointly determine which mtDNA mutations are able to persist on long-term
272 evolutionary timescales.
273
274 **DISCUSSION**
275 Major evolutionary transitions require cooperative interactions that incentivize group members to assume
276 the benefits of cooperation without the cost of reciprocating.[6-9] How might cheaters stably persist despite
277 deleteriously affecting the cooperators on which they depend? This question carries broad implications
278 ranging from evolutionary theory to the social and biomedical sciences, as prior exploration of cooperation
279 and cheating spans multiple systems and different levels of scale.[12,14,51] We sought to systematically compare
280 separate instances of cooperator-cheater dynamics, by leveraging a collection of selfish mitochondrial
281 genotypes existing in a uniform genetic and environmental background.
282
283 The selfish proliferation of mitochondrial mutations is responsible for a number of human diseases, affecting
284 an estimated 1 in 4,300 individuals, while an additional 1 in 200 healthy humans carry potentially disease-
285 causing mitochondrial mutations.[46] The same mutation may thus cause disease in one individual but not
286 another, due to variation in mutant frequency.[45,46] Consistent with this, disease-causing mutations vary
287 substantially in their ability to propagate from mother to offspring.[43,52] Predicting the inheritance and
288 development of mtDNA-associated disorders therefore requires a deep understanding of the underlying
289 evolutionary forces, and how they explain observed mutant frequencies. To this end, prior work generally
290 consists of either theoretical modeling or empirical study of mitochondrial mutations,[29,43,53-55] making it
291 difficult to integrate theory with experiment. Although some modeling studies incorporate empirical
292 data,[29,55-57] these focus on heteroplasmy dynamics within organisms, or within parent-progeny lineages,
293 making it difficult to combine the levels of selection into a complete evolutionary picture. To address these
294 challenges, we developed a hybrid approach that integrates theoretical modeling with experiments designed
295 to individually probe the levels of selection and the mutant frequency distribution.

296

297 The variant *uaDf5* is an exemplary model selfish mitochondrial genome, undergoing positive intra-
298 organismal selection at the expense of host fitness.[26,30,32,34-36,38] We expand the understanding of *uaDf5* in
299 numerous key ways. Prior studies have found that *uaDf5* proliferates not merely in spite of, but at least partly
300 *because* of, its negative effect on mitochondrial function.[32,34,36] Conversely, hosts are equipped with
301 mechanisms that limit *uaDf5* proliferation.[32,34,36,37,39] Together, these findings suggest opposing selection
302 forces at the intra-organismal level, in addition to organismal selection. Consistent with this, and with
303 previous reporting,[26,38] our modeling results confirm negative frequency-dependent selection for *uaDf5*, with
304 rising frequency leading to loss of its intra-organismal advantage, in addition to an organismal fitness cost.
305 More strikingly, we establish theoretically that the shape of the mutant frequency distribution contains
306 information about the underlying evolutionary forces. Thus, using *uaDf5* data, we show how the combination
307 of multilevel selection and genetic drift explains a previously observed peculiarity, namely the skewed
308 frequency distribution that concentrates most individuals toward the high end.[34]

309

310 How generalizable are the results concerning *uaDf5*? To answer this, we expanded our analysis to other
311 stably propagating heteroplasmies, each of which features a mutation known to deleteriously affect at least
312 one essential gene. Like *uaDf5*, some variants persist over time despite a heavy organismal fitness cost, due
313 to a strong intra-organismal advantage. These dynamics can be observed in three of the five
314 heteroplasmies—*uaDf5*, *mptDf2*, and *mpt4*—and are remarkably consistent with recent mammalian work.
315 For example, some mtDNA mutations in mice and humans rise in frequency from parents to offspring, in a
316 manner consistent with negative frequency-dependent selection,[43] suggesting a cheating behavior in human
317 mitochondrial disease similar to our findings. For some variants, however, we find no apparent organismal
318 selection, despite deletions in respiratory genes in the mutant genomes. This is true for *mpt2* and possibly
319 *mptDf3*, containing deletions in the genes *ND5* (ETC complex I) and cytochrome b (complex III), respectively,
320 although *mptDf3* results are consistent with a mild organismal fitness cost. How might a lineage lacking an

321 essential gene stably persist with no empirically observed fitness effects? Our modeling shows that a mutant
322 genome evade organismal selection via intra-organismal balancing selection, in which the mutant genome
323 loses its advantage at a frequency where the organismal fitness cost is negligible. One possible molecular
324 basis is that some mutant genomes are more vulnerable to cheater-suppression mechanisms, namely
325 mitochondrial autophagy, consistent with prior empirical work.[34,36,37,39,58-60] Alternatively, the dynamics of
326 mitochondrial fission and fusion may permit the diffusion of gene products throughout the mitochondrial
327 network, resulting in the genetic complementation of a mutation by nearby wildtype genomes. In either case,
328 such scenarios may enable a mutation to persist in a heteroplasmic state by remaining neutral or nearly
329 neutral at the organismal level.
330
331 We note two key limitations of this study, which easily serve as a basis for future work. First, in addition to
332 opposing selection forces, the introduction of selfish genomes by *de novo* mutation, a factor not considered
333 in this study, suggests that selfish mitochondrial genome dynamics represent a persistent phenomenon.
334 Consistent with this, previous mutation-accumulation experiments have identified selfish mtDNA variants in
335 *C. elegans* and the closely related species *C. briggsae*.[25,61] Together with our study, these findings suggest that
336 a heteroplasmic state may evolutionarily persist by a balance of selection forces, recurring reintroduction of
337 selfish mtDNA, or a combination of these factors.
338
339 Conditions beyond the mitochondria represent a second limitation. While our study employs a single host
340 genotype, previous research shows the nuclear genome to influence heteroplasmy dynamics. For example,
341 genetic regulators of mitochondrial biogenesis in response to stress, such as ATFS-1 and FoxO (DAF-16 in *C.*
342 *elegans*), as well as expression level of mtDNA replication machinery, are important determinants of selfish
343 mtDNA propagation.[26,32,34,36,41] Moreover, proteins with a more direct role in mitochondrial biogenesis and
344 mtDNA replication, such as POLG and the mtDNA-associated protein TFAM, or that promote binding of
345 replication machinery to mtDNA, reportedly mediate selfish mtDNA proliferation.[30,32,36] Conversely, genes

346 involved in mitochondrial fission and autophagy reportedly contribute to intra-organismal selection *against*
347 mutant mtDNA.[34,36,37,39,58-60] Given these findings, we propose that host genotypes and environmental factors,
348 especially those linking physiological stress with mtDNA replication and turnover, will be important
349 determinants of the cooperator-cheater dynamics described here and should be considered in future
350 research.
351
352 **METHODS**
353 **Nematode husbandry**
354 *C. elegans* strains used in this study were maintained on 60-mm standard nematode growth medium (NGM)
355 plates (for measuring intra-organismal selection), or 100-mm NGM plates (for measuring organismal
356 selection), seeded with live OP50-strain *E. coli* bacteria as a food source. Nematode strains were incubated
357 at 20°C. In addition to the Bristol wildtype strain and the heteroplasmic *uaDf5* strain featured in prior
358 work,[26] five additional *C. elegans* strains were used in this study. These consisted of heteroplasmic mutant
359 genomes *mptDf2*, *mpt4*, *mpt2*, and *mptDf3*, each crossed into the nuclear background of the Bristol strain.
360
361 **Nuclear genome exchange in heteroplasmic strains**
362 To ensure that our analysis was not confounded by variation in the nuclear genome, we completely
363 exchanged the nuclear genome of each heteroplasmic strain with the nuclear genome of wildtype (Bristol
364 strain) *C. elegans*, using a previously published unigametic inheritance method.[62] Thus, all heteroplasmic
365 strains used in this study have identical nuclear backgrounds. Briefly, each heteroplasmic strain was
366 crossed to the *gpr-1* over-expression strain PD2220 following Mendelian genetics. Next, hermaphrodites of
367 the stable *gpr-1* over-expression heteroplasmy strains were crossed to wildtype males. Non-Mendelian
368 hermaphrodite progeny from these crosses in which the paternal nuclear background is unigametically
369 inherited in the germline cell lineage (determined by pharyngeal mosaic patterning) were individually

370 propagated. Stock strains were established from the progeny of these animals as they have a complete
371 wildtype nuclear genomic background and retain the given heteroplasmy.
372
373 **DNA preparation**
374 To prepare animals for quantification of mutant mtDNA frequency, nematodes were transferred to sterile
375 PCR tubes or 96-well PCR plates containing lysis buffer with 100 μg/mL proteinase K. Lysis buffer
376 consisted of 50 mM KCl, 10 mM Tris pH 8.3, 2.5 mM $MgCl_2$, 0.45% Tween 20, 0.45% NP-40 (IGEPAL), and
377 0.01% gelatin, in deionized water. Volume of lysis buffer varied by worm count: 10 μL for individual adults
378 of the parent generation and 20 μL for pooled adult progeny for measuring intra-organismal selection, and
379 50 μL for pooled animal lysates from the competition experiments for measuring organismal selection.
380 After transferring worms to lysis buffer, each tube or plate was immediately sealed and incubated at -80°C
381 for 10 minutes to rupture nematode cuticles, followed by lysis incubation at 60°C for 60 minutes (90
382 minutes for pooled nematodes), and then at 95°C for 15 minutes to inactivate the proteinase K. Nematode
383 lysates were then kept at -20°C for stable long-term storage until being used for genotyping and
384 quantification.
385
386 **Quantifying mtDNA genotype frequencies**
387 Mutant mtDNA frequencies were quantified as described previously for *uaDf5*,[26] using droplet digital PCR
388 (ddPCR). Nematodes were lysed as described above and diluted in nuclease-free water with a dilution
389 factor varying depending on nematode concentration: 200x for single adults, 1000x for pooled adults
390 (intra-organismal selection experiment), and 20,000x for pooled nematodes of mixed age (organismal
391 selection experiment). For PCR amplification, 5 μL of diluted lysate was combined with 0.25 μL of 10-μM of
392 each oligonucleotide primer as needed depending on genotype:
393
394 *mptDf2*:

395 Forward 1: 5'-GGATTGGCAGTTTGATTAGAGAG-3'

396 Reverse 1: 5'-AAGTAACAAACACTAAAACTCCCAAC-3'

397 Forward 2: 5'-CGTGCTTATTTTTCGGCTGC-3'

398 Reverse 2: 5'-CTTTAACACCTGTTGGCACTG-3'

399 *mpt4*:

400 Forward 1: 5'-CGGTGGTTTTGGTAACTG-3'

401 Reverse 1: 5'-TCATAGTGTAACACCCGTGAAAATCC-3'

402 Forward 2: 5'-TGATCCAAGAACTGGAGGTAATC-3'

403 Reverse 2: 5'-CCTGTTGGCACTGCAATAAC-3'

404 *mpt2*:

405 Forward 1: 5'-GAAGAAGGTGGTAGCCTTGAGGAC-3'

406 Reverse 1: 5'-CGTATAAGAAAAGTCTTGGGATGTTAAG-3'

407 Forward 2: 5'-GGATTAATTTTCTCAAGGGGTGCTG-3'

408 Reverse 2: 5'-CTTTTTCAAAGACGAAAACTGTAACC-3'

409 *mptDf3*:

410 Forward 1: 5'-CCCTGAAGAGGCTAAGAATATTAGG-3'

411 Reverse 1: 5'-GGCAATGTCACCAACATCC-3'

412 Reverse 2: 5'-CCCAATACAATAACTAGAATAGCTCACG-3'

413

414 Mixtures of dilute lysate and primer were combined with 12.5 μL of Bio-Rad QX200™ ddPCR EvaGreen

415 Supermix and nuclease-free water to a volume of 25 μL in Eppendorf™ 96-well twin.tec™ PCR plates.

416 Droplet generation and PCR amplification were performed according to manufacturer protocol. Wildtype

417 and mutant-specific primers were combined in the same reaction, and each droplet was scored as

418 containing either wildtype or mutant mtDNA using the 2-dimensional (518 nm and 554 nm dual-

419 wavelength) clustering plot option in the Bio-Rad QuantaSoft™ program.

420

421 **Intra-organismal selection assay**

422 The strength of intra-organismal (within-host) selection on mutant mtDNA was measured longitudinally
423 across isolated parent-progeny lineages, as previously described.[26] Briefly, multiple L4-stage (late larval)
424 heteroplasmic animals were picked at random under a dissecting microscope from stock populations
425 carrying each heteroplasmy that had been crossed into the Bristol strain (wildtype) nuclear background.
426 These larvae were transferred to fresh NGM plates seeded with live OP50 *E. coli* bacteria as a food source
427 and incubated for 2 days at 20°C to allow adult maturation. The day-2 adults were individually segregated
428 by transferring each onto a fresh food plate and incubated for 4 hours at 20°C to produce embryos that are
429 age-synchronized to within a four-hour window. Each parent was then individually lysed. After 4 days of
430 continued incubation at 20°C, the progeny had progressed from embryos to day-2 adults, reaching the
431 same age at which their respective parents were lysed. Adult progeny were lysed at this point to obtain
432 progeny that are age-matched to their parents, to control for age-dependent differences in mutant mtDNA
433 levels. Progeny from each parent were lysed in pools of 3 to minimize the confounding effect of random
434 drift. Each parent-progeny lineage was individually segregated from the rest, to ensure that mutant mtDNA
435 frequency from each progeny lysate was being compared with that of its own respective parent, thereby
436 minimizing the confounding effect of competition between lineages (organismal selection). Mutant mtDNA
437 frequency of parents and progeny was determined for each heteroplasmy using ddPCR as described above,
438 across multiple replicate parent-progeny lineages for statistical power.

439

440 **Experimental evolution (organismal selection)**

441 Selection against mutant mtDNA that occurs strictly at the level of host fitness was measured using an
442 organismal competition experiment similarly to the experiment previously described [26]. Briefly, for each
443 mutant mtDNA variant, heteroplasmic nematodes carrying mutant mtDNA in the Bristol nuclear
444 background were combined with Bristol-strain nematodes on 10-cm NGM plates seeded with live OP50 *E.*

coli bacteria as a food source. Approximately 500 nematodes were transferred to each plate. In addition to 4 replicate competition lines for each heteroplasmy, 4 non-competing control lines were established by transferring only heteroplasmic animals onto their own food plates, with no homoplasmic-wildtype animals to compete against. Every 3 days, the generation for each experimental line was reset; nematodes were washed off the plates using M9 buffer into a sterile 1.7 mL collection tube. Approximately 500 animals of mixed age from each line were transferred to a fresh food plate. Another 500 nematodes were lysed together in a single pooled lysate. This experiment was continued for 6 consecutive generations.

Population genetic model

To treat the evolutionary dynamics of multilevel selection and drift in a theoretical population genetic framework, we constructed a model that couples a stochastic, frequency-dependent Wright-Fisher model for the evolution of mutant mtDNA frequencies within individuals together with a frequency-independent, deterministic model of organismal competition. The intra-organismal fitness function measures the fitness of mutant mtDNA relative to wildtype mtDNA within an individual. We model the intra-organismal fitness function as a sigmoid function of mutant frequency:

$$w_{intra}(z) = \delta\left(\frac{1}{1+e^{\gamma z+\varepsilon}}\right),$$

where parameters δ, γ, and ε control the overall scale of fitness variation, the degree of frequency-dependence, and the position of the inflection point, respectively, as a function of mutant mtDNA frequency. The organismal fitness function is modeled in terms of the fitness cost of carrying a selfish mitochondrial genome at frequency z:

$$w_{org}(z) = 1 - \frac{\int_0^z x^{\alpha-1}(1-x)^{\beta-1}dx}{\int_0^1 x^{\alpha-1}(1-x)^{\beta-1}dx}.$$

This is identical to the complementary cumulative distribution function of a beta distribution with parameters α and β, so that we necessarily have $w_{org}(0)=1$ (wildtype individuals have fitness 1) and $w_{org}(1)=0$ (individuals fixed for the selfish mutant are either sterile or nonviable). Importantly, when β=1

this expression reduces to $w_{org}(z)=1-z^{\alpha}$, corresponding to a fitness defect that scales as z to the power α, or a linear fitness decline when both α=1 and β=1. This expression can thus encompass a variety of simple models for how mutant mtDNA frequency impacts organismal fitness, in addition to more complex threshold-like models. Note also that while the organismal fitness function depends on the mutant mtDNA frequency of the individual, in our model organismal selection is frequency-independent in that the fitness of an individual does not depend on the composition of the remainder of the population.

To combine this intra-organismal and organismal selection with stochastic inheritance arising from intra-organismal genetic drift, we construct an N+1 by N+1 matrix,

$$M(i,j) = p\left(j; N, \frac{i w_{intra}(i/N)}{i w_{intra}(i/N) + (N-i)}\right) \times w_{org}(j/N),$$

where the indices i and j run from 0 to N, $p(j; N, q)$ is the binomial probability of a total of j successes out of N attempts with expected mutant mtDNA frequency q among the offspring of a parent with mutant mtDNA frequency i/N (which itself is given by $i\, w_{intra}(i/N)$ / ($i\, w_{intra}(i/N)$+(N–i))). Thus $M(i,j)$ gives the expected proportion of progeny with a mutant mtDNA frequency of j/N for a parent with a mutant mtDNA frequency i/N. Writing the probability distribution of heteroplasmic mutant frequencies at time t as a length N vector f_t, the time evolution of this probability distribution is given by:

$$f_{t+1}^T = \frac{f_t^T M'}{f_t^T M' \mathbf{1}_N},$$

where M' is the N by N principal submatrix of M obtained by omitting the zeroth row and column, and $\mathbf{1}_N$ is the length N vector of all 1s. By the Perron-Frobenius theorem,[63] as t goes to infinity, f_t converges to a stable distribution f^* given by the dominant left eigenvector of M'. The corresponding eigenvalue gives the expected number of heteroplasmic offspring per heteroplasmic parent under the stable distribution f^*. The expected number of wildtype offspring per heteroplasmic parent (spontaneous reversion from heteroplasmy to homoplasmic-wildtype) under the stable distribution f^* is given by:

$$r = (f_{N+1}^*)^T M \boldsymbol{e}_0,$$

where f^*_{N+1} is the vector of length N+1 whose zeroth entry is 0 and whose remaining entries are given by f^*, and $\boldsymbol{e}_0$ is the length N+1 vector whose zeroth entry is 1 and whose remaining entries are 0.

Maximum likelihood inference

We estimate the model parameters for each mutant mtDNA genotype using a joint maximum likelihood approach (that is, a combined fit to the data from the intra-organismal selection experiment, organismal selection experiment, and the sampled stable mutant frequency distribution) with parameter uncertainty assessed via a parametric bootstrap approach. Model fitting was conducted using a custom Python script (code available at https://github.com/bgitschlag/MiSelf).

For intra-organismal selection experiment, we model the mutant frequency within the progeny, $z_{obs,t+1}$, as a function of the mutant frequency z_t of the parent as:

$$z_{obs,t+1} = \frac{z_t w_{intra}(z_t)}{z_t w_{intra}(z_t) + (1 - z_t)} + e_{intra},$$

where e_{intra} is a normally distributed random variable with mean 0 and variance given by the free parameter σ^2_{intra}. For the organismal selection experiment, the population-wide fraction of heteroplasmic individuals, ϕ, changes across generations due to both the organismal fitness cost and spontaneous loss of the mutant genome, r. At each generation, ϕ experiences a growth rate, relative to the wildtype, of $\kappa=(f^*)^T M' \mathbf{1}_N$, and a rate of mutant loss r, which collectively determine the fraction of heteroplasmic individuals in each subsequent generation:

$$\phi_{t+1} = \frac{\phi_t \kappa}{\phi_t \kappa + \phi_t r + (1 - \phi_t)}.$$

Because in the special case where mutant frequency declines solely due to organismal selection (that is, r=0), $\ln(\phi/(1-\phi))$ decreases linearly in time, we model ϕ on a log-odds scale:

$$\ln \frac{\phi_{obs,t}}{1 - \phi_{obs,t}} = \ln \frac{\phi_t}{1 - \phi_t} + e_{org},$$

where $\phi_{obs,t}$ is the empirically observed ϕ at time t, e_{org} is a normally distributed random variable with mean 0 and variance given by the free parameter σ^2_{org}. In addition, the initial frequency ϕ_0 is also inferred as a free parameter. Finally, to determine the likelihood of draws from f^*, we construct a continuous analog of the discrete distribution f^* by applying a Gaussian smoother and calculating the likelihood under the resulting probability density function. Specifically, we convolve the discrete distribution described by f^* with a Gaussian random variable with mean 0 and standard deviation $1/N$.

In summary, our statistical model has free parameters, N, δ, γ, and ε (controlling intra-organismal selection and drift), σ^2_{intra} (controlling the noise variance of the intra-organismal selection experiment), α and β (controlling the form of organismal selection), and σ^2_{org} (controlling the noise variance in the organismal selection experiment). Because all of these parameters are continuous except for N, for each possible N from 10 to 100 we numerically maximized the likelihood with respect to all other parameters. We then selected the value of N that maximized the likelihood.

To estimate our confidence in these parameter estimates, we performed parametric bootstrapping by simulating 100 data sets per genotype, using the sample sizes, maximum-likelihood population-genetic parameters, and error estimates for the corresponding empirical data set. Specifically, to simulate the intra-organismal selection experiment, parent mutant frequencies z_t were randomly drawn from the Gaussian smoothed version of f^* and then the corresponding progeny frequencies z_{t+1} were randomly drawn according to our inferred Wright-Fisher process. To simulate the organismal selection experiment, the expected heteroplasmic fraction ϕ_t at each generational time t was calculated using the maximum-likelihood estimate of ϕ_0 combined with the r and κ values determined from our maximum-likelihood estimates. We then converted these expected fractions ϕ_t onto a log odds scale, added Gaussian noise with variance σ^2_{org}, and finally converted them back to a frequency scale. The samples from the mutant frequency distribution were simulated by drawing from the Gaussian smoothed version of f^* with sample

sizes equaling that of the corresponding empirical data set. For each simulated data set, model parameters were re-estimated using the same maximum-likelihood approach described above. However, for some bootstrap simulations the maximum likelihood estimate of N was realized at or near the upper boundary of our search space. In such cases we thus examined larger values of N, starting at N=125 and increasing by powers of $\sqrt{2}$ (125, 177, 250, 354, 500, etc.). We continued in this manner until the maximum-likelihood estimate of N reached a peak, defined as a maximum-likelihood N that is no longer among the 2 consecutive largest values of N examined so far, or until reaching a maximum-likelihood N=1,000, at which point we concluded that the magnitude of drift approximates that of the high-N limit.

DATA AVAILABILITY

Data from experiments measuring selection on *uaDf5* were previously published.[26] These and other experimental data encompassing the remaining four genotypes are included as Source Data files in this study.

CODE AVAILABILITY

All code is publicly available at https://github.com/bgitschlag/MiSelf

REFERENCES

1 Szathmary, E. & Smith, J. M. The major evolutionary transitions. *Nature* **374**, 227-232, doi:10.1038/374227a0 (1995).

2 Vanchurin, V., Wolf, Y. I., Katsnelson, M. I. & Koonin, E. V. Toward a theory of evolution as multilevel learning. *Proc Natl Acad Sci U S A* **119**, doi:10.1073/pnas.2120037119 (2022).

3 West, S. A., Fisher, R. M., Gardner, A. & Kiers, E. T. Major evolutionary transitions in individuality. *Proc Natl Acad Sci U S A* **112**, 10112-10119, doi:10.1073/pnas.1421402112 (2015).

4 Carmel, Y. & Shavit, A. Operationalizing evolutionary transitions in individuality. *Proc Biol Sci* **287**, 20192805, doi:10.1098/rspb.2019.2805 (2020).

5 Michod, R. E. The group covariance effect and fitness trade-offs during evolutionary transitions in individuality. *Proc Natl Acad Sci U S A* **103**, 9113-9117, doi:10.1073/pnas.0601080103 (2006).

6 Ghoul, M., Griffin, A. S. & West, S. A. Toward an evolutionary definition of cheating. *Evolution* **68**, 318-331, doi:10.1111/evo.12266 (2014).

7 Gore, J., Youk, H. & van Oudenaarden, A. Snowdrift game dynamics and facultative cheating in yeast. *Nature* **459**, 253-256, doi:10.1038/nature07921 (2009).

572 8 Sexton, D. J. & Schuster, M. Nutrient limitation determines the fitness of cheaters in bacterial
573 siderophore cooperation. *Nat Commun* **8**, 230, doi:10.1038/s41467-017-00222-2 (2017).
574 9 Strassmann, J. E., Zhu, Y. & Queller, D. C. Altruism and social cheating in the social amoeba
575 Dictyostelium discoideum. *Nature* **408**, 965-967, doi:10.1038/35050087 (2000).
576 10 Aktipis, C. A. *et al.* Cancer across the tree of life: cooperation and cheating in multicellularity.
577 *Philos Trans R Soc Lond B Biol Sci* **370**, doi:10.1098/rstb.2014.0219 (2015).
578 11 Bravo Nunez, M. A., Nuckolls, N. L. & Zanders, S. E. Genetic Villains: Killer Meiotic Drivers. *Trends*
579 *Genet* **34**, 424-433, doi:10.1016/j.tig.2018.02.003 (2018).
580 12 Riehl, C. & Frederickson, M. E. Cheating and punishment in cooperative animal societies. *Philos*
581 *Trans R Soc Lond B Biol Sci* **371**, 20150090, doi:10.1098/rstb.2015.0090 (2016).
582 13 Zanders, S. E. & Unckless, R. L. Fertility Costs of Meiotic Drivers. *Curr Biol* **29**, R512-R520,
583 doi:10.1016/j.cub.2019.03.046 (2019).
584 14 Patten, M. M., Schenkel, M. A. & Agren, J. A. Adaptation in the face of internal conflict: the
585 paradox of the organism revisited. *Biol Rev Camb Philos Soc*, doi:10.1111/brv.12983 (2023).
586 15 de Vargas Roditi, L., Boyle, K. E. & Xavier, J. B. Multilevel selection analysis of a microbial social
587 trait. *Mol Syst Biol* **9**, 684, doi:10.1038/msb.2013.42 (2013).
588 16 Dobata, S. & Tsuji, K. Public goods dilemma in asexual ant societies. *Proc Natl Acad Sci U S A* **110**,
589 16056-16060, doi:10.1073/pnas.1309010110 (2013).
590 17 Fiegna, F. & Velicer, G. J. Competitive fates of bacterial social parasites: persistence and self-
591 induced extinction of Myxococcus xanthus cheaters. *Proc Biol Sci* **270**, 1527-1534,
592 doi:10.1098/rspb.2003.2387 (2003).
593 18 Havird, J. C. *et al.* Selfish Mitonuclear Conflict. *Curr Biol* **29**, R496-R511,
594 doi:10.1016/j.cub.2019.03.020 (2019).
595 19 Munoz-Gomez, S. A. *et al.* Site-and-branch-heterogeneous analyses of an expanded dataset
596 favour mitochondria as sister to known Alphaproteobacteria. *Nat Ecol Evol* **6**, 253-262,
597 doi:10.1038/s41559-021-01638-2 (2022).
598 20 Sagan, L. On the origin of mitosing cells. *J Theor Biol* **14**, 255-274, doi:10.1016/0022-
599 5193(67)90079-3 (1967).
600 21 Castellani, C. A., Longchamps, R. J., Sun, J., Guallar, E. & Arking, D. E. Thinking outside the nucleus:
601 Mitochondrial DNA copy number in health and disease. *Mitochondrion* **53**, 214-223,
602 doi:10.1016/j.mito.2020.06.004 (2020).
603 22 Chen, Z. *et al.* Mitochondrial DNA segregation and replication restrict the transmission of
604 detrimental mutation. *J Cell Biol* **219**, doi:10.1083/jcb.201905160 (2020).
605 23 Birky, C. W. Relaxed and Stringent Genomes - Why Cytoplasmic Genes Dont Obey Mendels Laws.
606 *J Hered* **85**, 355-365, doi:DOI 10.1093/oxfordjournals.jhered.a111480 (1994).
607 24 Chatre, L. & Ricchetti, M. Prevalent coordination of mitochondrial DNA transcription and
608 initiation of replication with the cell cycle. *Nucleic Acids Res* **41**, 3068-3078,
609 doi:10.1093/nar/gkt015 (2013).
610 25 Dubie, J. J., Caraway, A. R., Stout, M. M., Katju, V. & Bergthorsson, U. The conflict within: origin,
611 proliferation and persistence of a spontaneously arising selfish mitochondrial genome. *Philos*
612 *Trans R Soc Lond B Biol Sci* **375**, 20190174, doi:10.1098/rstb.2019.0174 (2020).
613 26 Gitschlag, B. L., Tate, A. T. & Patel, M. R. Nutrient status shapes selfish mitochondrial genome
614 dynamics across different levels of selection. *Elife* **9**, doi:10.7554/eLife.56686 (2020).

615 27 Klucnika, A. & Ma, H. A battle for transmission: the cooperative and selfish animal mitochondrial
616 genomes. *Open Biol* **9**, 180267, doi:10.1098/rsob.180267 (2019).
617 28 Leigh, E. G. When does the good of the group override the advantage of the individual? *Proc Natl*
618 *Acad Sci U S A* **80**, 2985-2989, doi:10.1073/pnas.80.10.2985 (1983).
619 29 Pereira, C. V., Gitschlag, B. L. & Patel, M. R. Cellular mechanisms of mtDNA heteroplasmy
620 dynamics. *Critical Reviews in Biochemistry and Molecular Biology*, 1-16,
621 doi:10.1080/10409238.2021.1934812 (2021).
622 30 Schwartz, A. Z. A. & Nance, J. Germline TFAM levels regulate mitochondrial DNA copy number
623 and mutant heteroplasmy in C. elegans. *MicroPubl Biol* **2023**,
624 doi:10.17912/micropub.biology.000727 (2023).
625 31 Schwartz, A. Z. A., Tsyba, N., Abdu, Y., Patel, M. R. & Nance, J. Independent regulation of
626 mitochondrial DNA quantity and quality in Caenorhabditis elegans primordial germ cells. *Elife* **11**,
627 doi:10.7554/eLife.80396 (2022).
628 32 Yang, Q. *et al.* LONP-1 and ATFS-1 sustain deleterious heteroplasmy by promoting mtDNA
629 replication in dysfunctional mitochondria. *Nat Cell Biol* **24**, 181-193, doi:10.1038/s41556-021-
630 00840-5 (2022).
631 33 Ahier, A. *et al.* Affinity purification of cell-specific mitochondria from whole animals resolves
632 patterns of genetic mosaicism. *Nat Cell Biol* **20**, 352-360, doi:10.1038/s41556-017-0023-x (2018).
633 34 Gitschlag, B. L. *et al.* Homeostatic Responses Regulate Selfish Mitochondrial Genome Dynamics
634 in C. elegans. *Cell Metab* **24**, 91-103, doi:10.1016/j.cmet.2016.06.008 (2016).
635 35 Liau, W. S., Gonzalez-Serricchio, A. S., Deshommes, C., Chin, K. & LaMunyon, C. W. A persistent
636 mitochondrial deletion reduces fitness and sperm performance in heteroplasmic populations of
637 C. elegans. *BMC Genet* **8**, 8, doi:10.1186/1471-2156-8-8 (2007).
638 36 Lin, Y. F. *et al.* Maintenance and propagation of a deleterious mitochondrial genome by the
639 mitochondrial unfolded protein response. *Nature* **533**, 416-419, doi:10.1038/nature17989
640 (2016).
641 37 Meshnik, L. *et al.* Mutant C. elegans mitofusin leads to selective removal of mtDNA heteroplasmic
642 deletions across generations to maintain fitness. *BMC Biol* **20**, 40, doi:10.1186/s12915-022-
643 01241-2 (2022).
644 38 Tsang, W. Y. & Lemire, B. D. Stable heteroplasmy but differential inheritance of a large
645 mitochondrial DNA deletion in nematodes. *Biochem Cell Biol* **80**, 645-654 (2002).
646 39 Valenci, I., Yonai, L., Bar-Yaacov, D., Mishmar, D. & Ben-Zvi, A. Parkin modulates heteroplasmy of
647 truncated mtDNA in Caenorhabditis elegans. *Mitochondrion* **20**, 64-70,
648 doi:10.1016/j.mito.2014.11.001 (2015).
649 40 Capps, G. J., Samuels, D. C. & Chinnery, P. F. A model of the nuclear control of mitochondrial DNA
650 replication. *J Theor Biol* **221**, 565-583 (2003).
651 41 Chiang, A. C., McCartney, E., O'Farrell, P. H. & Ma, H. A Genome-wide Screen Reveals that
652 Reducing Mitochondrial DNA Polymerase Can Promote Elimination of Deleterious Mitochondrial
653 Mutations. *Curr Biol* **29**, 4330-4336 e4333, doi:10.1016/j.cub.2019.10.060 (2019).
654 42 Taylor, R. W. & Turnbull, D. M. Mitochondrial DNA mutations in human disease. *Nat Rev Genet*
655 **6**, 389-402, doi:10.1038/nrg1606 (2005).
656 43 Zhang, H. *et al.* Mitochondrial DNA heteroplasmy is modulated during oocyte development
657 propagating mutation transmission. *Sci Adv* **7**, eabi5657, doi:10.1126/sciadv.abi5657 (2021).

658 44 Chiaratti, M. R. & Chinnery, P. F. Modulating mitochondrial DNA mutations: factors shaping
659 heteroplasmy in the germ line and somatic cells. *Pharmacol Res* **185**, 106466,
660 doi:10.1016/j.phrs.2022.106466 (2022).
661 45 Schon, E. A., DiMauro, S. & Hirano, M. Human mitochondrial DNA: roles of inherited and somatic
662 mutations. *Nat Rev Genet* **13**, 878-890, doi:10.1038/nrg3275 (2012).
663 46 Stewart, J. B. & Chinnery, P. F. The dynamics of mitochondrial DNA heteroplasmy: implications
664 for human health and disease. *Nat Rev Genet* **16**, 530-542, doi:10.1038/nrg3966 (2015).
665 47 Konrad, A. *et al.* Mitochondrial Mutation Rate, Spectrum and Heteroplasmy in Caenorhabditis
666 elegans Spontaneous Mutation Accumulation Lines of Differing Population Size. *Mol Biol Evol* **34**,
667 1319-1334, doi:10.1093/molbev/msx051 (2017).
668 48 Patwa, Z. & Wahl, L. M. The fixation probability of beneficial mutations. *J R Soc Interface* **5**, 1279-
669 1289, doi:10.1098/rsif.2008.0248 (2008).
670 49 Teterina, A. A. *et al.* Genomic diversity landscapes in outcrossing and selfing Caenorhabditis
671 nematodes. *PLoS Genet* **19**, e1010879, doi:10.1371/journal.pgen.1010879 (2023).
672 50 Stiernagle, T. Maintenance of C. elegans. *WormBook*, 1-11, doi:10.1895/wormbook.1.101.1
673 (2006).
674 51 Shou, W. Acknowledging selection at sub-organismal levels resolves controversy on pro-
675 cooperation mechanisms. *Elife* **4**, doi:10.7554/eLife.10106 (2015).
676 52 Wei, W. *et al.* Germline selection shapes human mitochondrial DNA diversity. *Science* **364**,
677 doi:10.1126/science.aau6520 (2019).
678 53 Bergstrom, C. T. & Pritchard, J. Germline bottlenecks and the evolutionary maintenance of
679 mitochondrial genomes. *Genetics* **149**, 2135-2146, doi:10.1093/genetics/149.4.2135 (1998).
680 54 Colnaghi, M., Pomiankowski, A. & Lane, N. The need for high-quality oocyte mitochondria at
681 extreme ploidy dictates mammalian germline development. *Elife* **10**, doi:10.7554/eLife.69344
682 (2021).
683 55 Johnston, I. G. & Burgstaller, J. P. Evolving mtDNA populations within cells. *Biochem Soc Trans* **47**,
684 1367-1382, doi:10.1042/BST20190238 (2019).
685 56 Giannakis, K., Broz, A. K., Sloan, D. B. & Johnston, I. G. Avoiding misleading estimates using mtDNA
686 heteroplasmy statistics to study bottleneck size and selection. *G3 (Bethesda)* **13**,
687 doi:10.1093/g3journal/jkad068 (2023).
688 57 Royrvik, E. C. & Johnston, I. G. MtDNA sequence features associated with 'selfish genomes'
689 predict tissue-specific segregation and reversion. *Nucleic Acids Res* **48**, 8290-8301,
690 doi:10.1093/nar/gkaa622 (2020).
691 58 Kandul, N. P., Zhang, T., Hay, B. A. & Guo, M. Selective removal of deletion-bearing mitochondrial
692 DNA in heteroplasmic Drosophila. *Nat Commun* **7**, 13100, doi:10.1038/ncomms13100 (2016).
693 59 Lieber, T., Jeedigunta, S. P., Palozzi, J. M., Lehmann, R. & Hurd, T. R. Mitochondrial fragmentation
694 drives selective removal of deleterious mtDNA in the germline. *Nature* **570**, 380-384,
695 doi:10.1038/s41586-019-1213-4 (2019).
696 60 Suen, D. F., Narendra, D. P., Tanaka, A., Manfredi, G. & Youle, R. J. Parkin overexpression selects
697 against a deleterious mtDNA mutation in heteroplasmic cybrid cells. *Proc Natl Acad Sci U S A* **107**,
698 11835-11840, doi:10.1073/pnas.0914569107 (2010).
699 61 Phillips, W. S. *et al.* Selfish Mitochondrial DNA Proliferates and Diversifies in Small, but not Large,
700 Experimental Populations of Caenorhabditis briggsae. *Genome Biol Evol* **7**, 2023-2037,
701 doi:10.1093/gbe/evv116 (2015).

62 Artiles, K. L., Fire, A. Z. & Frokjaer-Jensen, C. Assessment and Maintenance of Unigametic Germline Inheritance for C. elegans. *Dev Cell* **48**, 827-839 e829, doi:10.1016/j.devcel.2019.01.020 (2019).
63 Seneta, E. *Non-negative matrices and Markov chains*. Rev. print. edn, (Springer, 2006).

ACKNOWLEDGMENTS

The *uaDf5* strain was kindly provided by the Caenorhabditis Genetics Center (CGC). We thank O. Thompson and R. Waterston at the University of Washington for identifying the *mptDf2*, *mpt4*, *mpt2*, and *mptDf3* genotypes from the Million Mutation Project worm collection. We thank Patrick Abbot and Ann T. Tate of Vanderbilt University for valuable conceptual insights and guidance with experimental design. This work was supported by the NIH research project grants R01 GM123260 and R35 GM145378 (M.R.P.), Discovery Award (PR170792) from the Department of Defense's Congressionally Directed Medical Research Program (M.R.P.), the Vanderbilt University Medical Center Diabetes Research and Training Center Pilot & Feasibility Grant (M.R.P.), the NIH-sponsored Cellular, Molecular and Biochemical and Molecular Sciences Training Program (5T32GM008554-18, B.L.G.), the Ruth L. Kirschstein National Research Service Award Individual Predoctoral Fellowship (1F31GM125344, B.L.G.), R35 GM133613 (D.M.M.), an Alfred P. Sloan Research Fellowship and additional funding from the Simons Center for Quantitative Biology and Cold Spring Harbor Laboratory (D.M.M.).

AUTHOR CONTRIBUTIONS

B.L.G., D.M.M., and M.R.P. designed the study. B.L.G., C.V.P., and J.P.H. performed experiments to collect the data. B.L.G. and D.M.M. performed mathematical modeling. B.L.G., D.M.M., and M.R.P. analyzed the data. B.L.G. prepared the first manuscript draft. All authors revised and edited the manuscript.

COMPETING INTERESTS

The authors declare no competing interests.

ADDITIONAL INFORMATION

Correspondence should be addressed to Bryan L. Gitschlag or Maulik R. Patel.

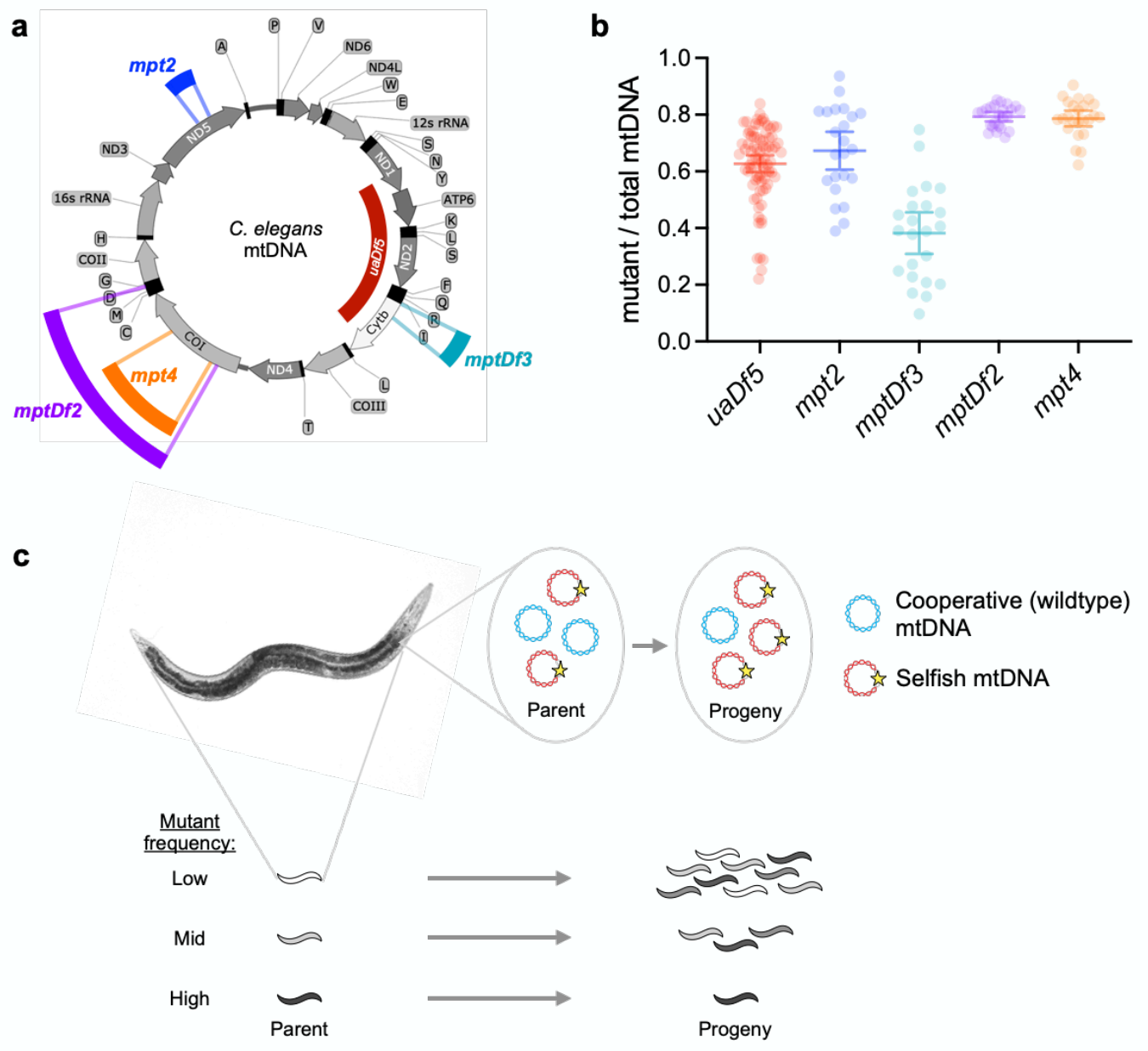

Figure 1: A collection of mutant mitochondrial genotypes stably persisting in a heteroplasmic state despite disruption of essential respiratory genes.

a, *C. elegans* mitochondrial genome, with the locations and sizes of mutations represented by the color-coded bars. **b**, distribution of heteroplasmic mutant frequencies for age-synchronized adult animals each carrying one of the mutations shown in **a**. Error bars indicate mean and 95% confidence interval of mean. **c**, schematic of multilevel selection, with a selfish mitochondrial genome undergoing positive intra-organismal (within-host) selection and negative organismal (between-host) selection. Shading indicates frequency of selfish mtDNA.

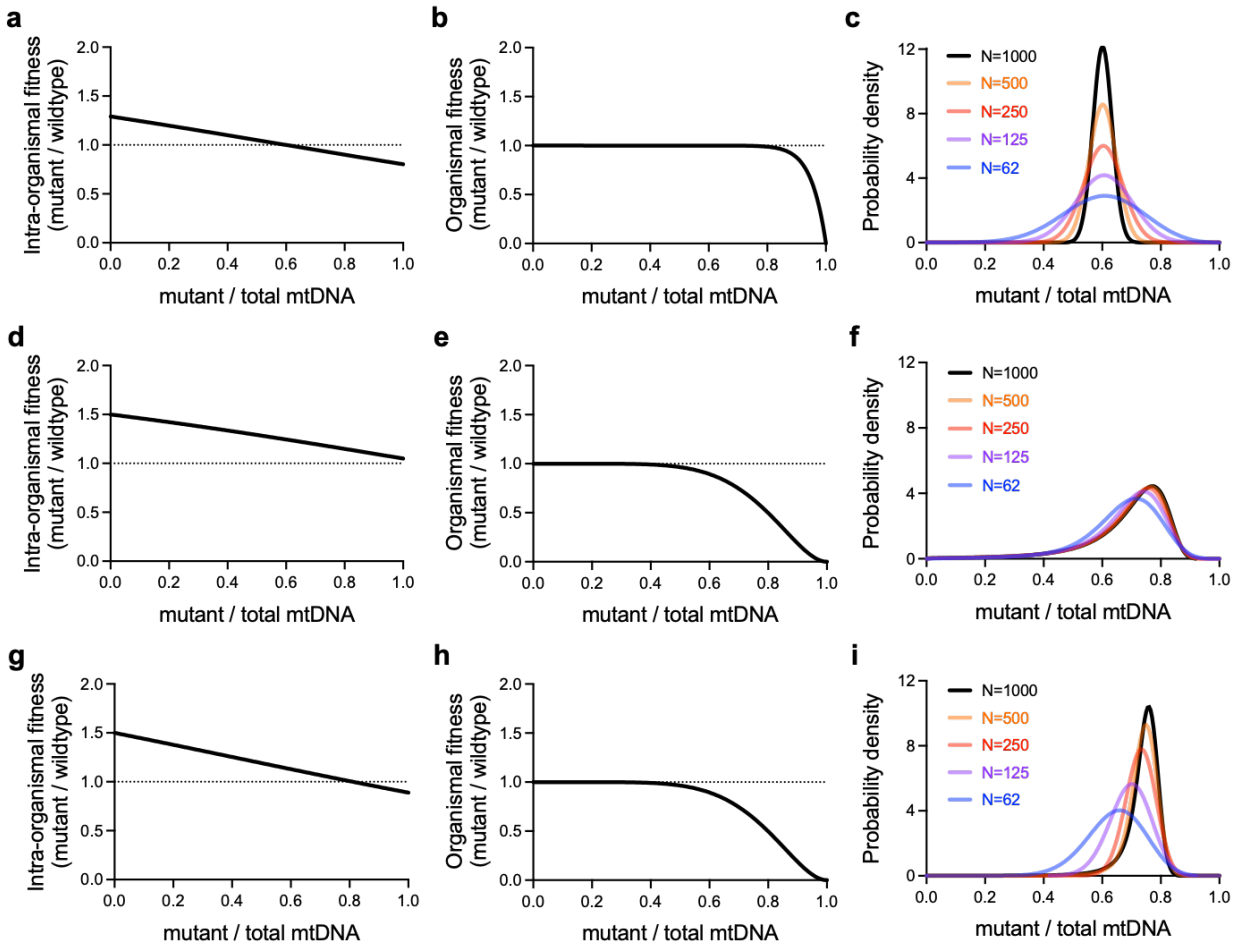

742

743 **Figure 2: Theoretical modeling reveals the stable maintenance of a selfish mitochondrial genome**
744 **through a variety of evolutionary mechanisms.**

745 **a-c**, the intra-organismal fitness advantage of a selfish mitochondrial genome (**a**) disappears at a frequency
746 too low for the genome to inflict a substantial organismal fitness cost (**b**). The selfish mtDNA is maintained
747 at a mean frequency set by balancing selection at the intra-organismal level, with neutral drift determining
748 the width of the mutant frequency distribution (**c**). **d-f**, a constitutive intra-organismal fitness advantage
749 (**d**) pushes mutant frequency into a range wherein it encounters increasing organismal fitness cost (**e**).
750 Multilevel selection can maintain a broad range of mutant frequencies (**f**), even when neutral drift is
751 minimal. **g-i**, the intra-organismal fitness advantage (**g**) disappears within approximately the same range of
752 mutant frequencies in which organismal fitness declines most rapidly (**h**). Changes in the strength of intra-
753 organismal genetic drift alter both the width and center of the distribution of selfish mtDNA frequencies (**i**).

754

755

756

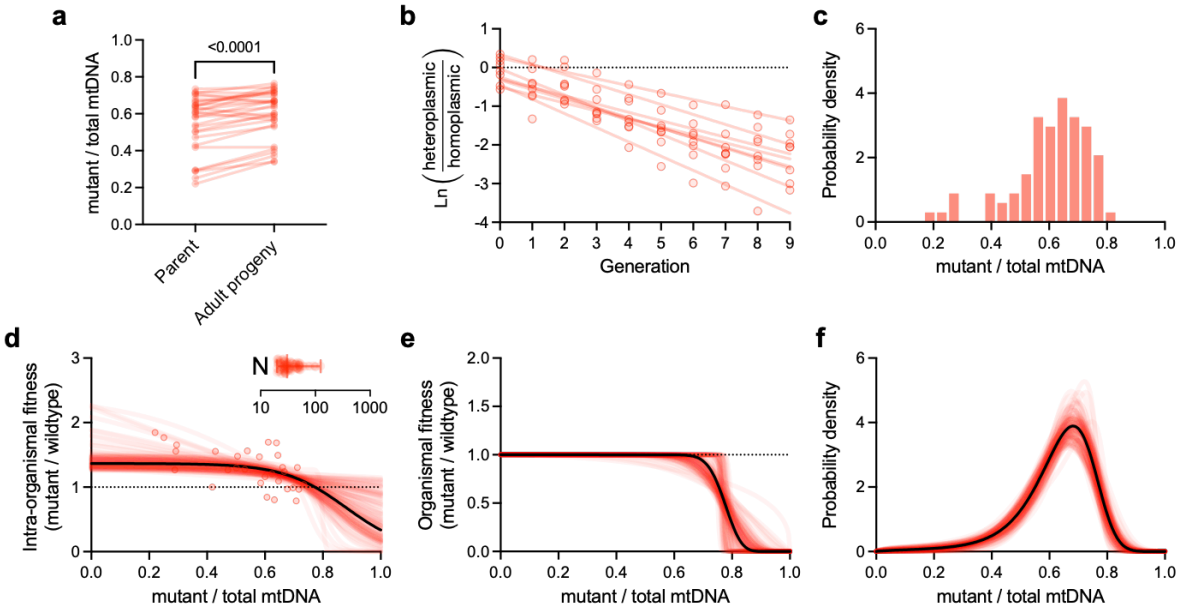

Figure 3: Integration of benchtop experimentation with theoretical modeling reveals the stable maintenance of a selfish mitochondrial genome via a combination of multilevel selection and neutral drift.

a, pairwise comparisons of mutant frequency (*uaDf5*) between parent and progeny for the purpose of measuring intra- organismal selection on a selfish mitochondrial genome (n=30). **b**, organismal selection against *uaDf5*, measured by directly competing heteroplasmic carriers of the selfish genome against homoplasmic (wildtype) animals on the same food plate, in a mixed population (n=8). **c**, histogram of mutant frequencies (n=81) of age-synchronized adults sampled from a heteroplasmic stock population. Data in **a-c** are taken from our prior study.[26] **d-f**, maximum-likelihood estimates of the intra-organismal (**d**) and organismal (**e**) fitness effects, each as a function of mutant frequency, and the most evolutionarily stable mutant frequency distribution (**f**). Each plot shows the maximum likelihood estimates corresponding to the empirical data represented in the top row (solid black line) and 100 simulated data sets for parametric bootstrapping (red lines) to visualize the confidence estimates for each plot. Model parameters specifying intra-organismal selection, organismal selection, and intra-organismal genetic drift (**d**, inset, bars indicate mean, lowest and highest values), were collectively estimated using a joint maximum likelihood approach that combines all 3 data sets (top row).

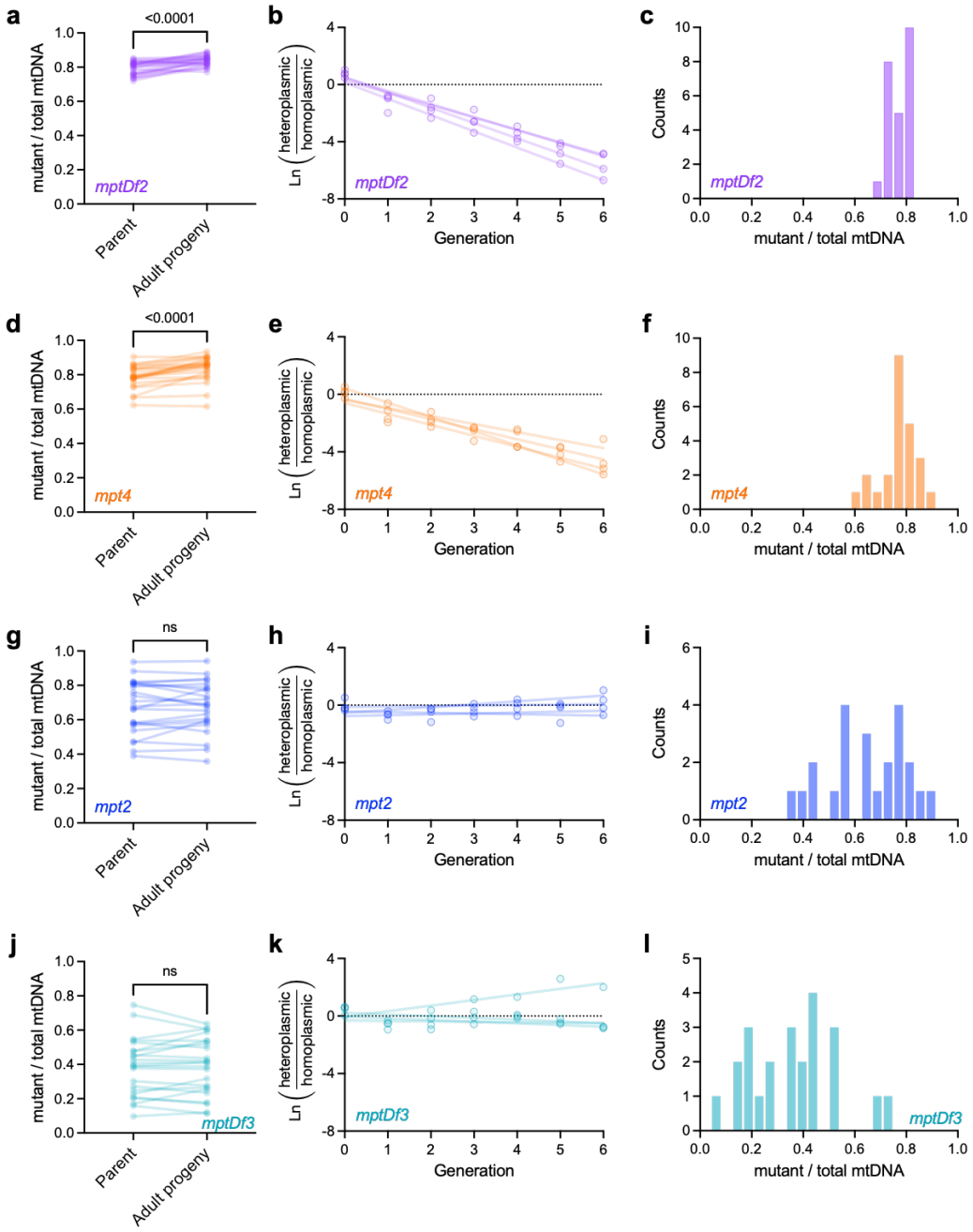

Figure 4: Measurements of intra-organismal selection, organismal selection, and mutant frequency distributions across a panel of putatively selfish mitochondrial genome variants.

a, *mptDf2* frequencies in isolated parent-progeny lineages (n=24) to measure intra-organismal selection, similar to Fig. 3d. **b**, relative proportions of *mptDf2* heteroplasmic versus homoplasmic-wildtype hosts per generation in populations of animals competing on the same food plate (n=4), to measure organismal selection. **c**, histogram of *mptDf2* frequencies in age- synchronized adults sampled from heteroplasmic stock populations (the same individuals used as parent data points in **a**). **d-f**, similar to **a-c** but for *mpt4* (**d**, n=24). **g-i**, similar to **a-c** but for *mpt2* (**g**, n=23). **j-l**, similar to **a-c** but for *mptDf3* (**j**, n=23).

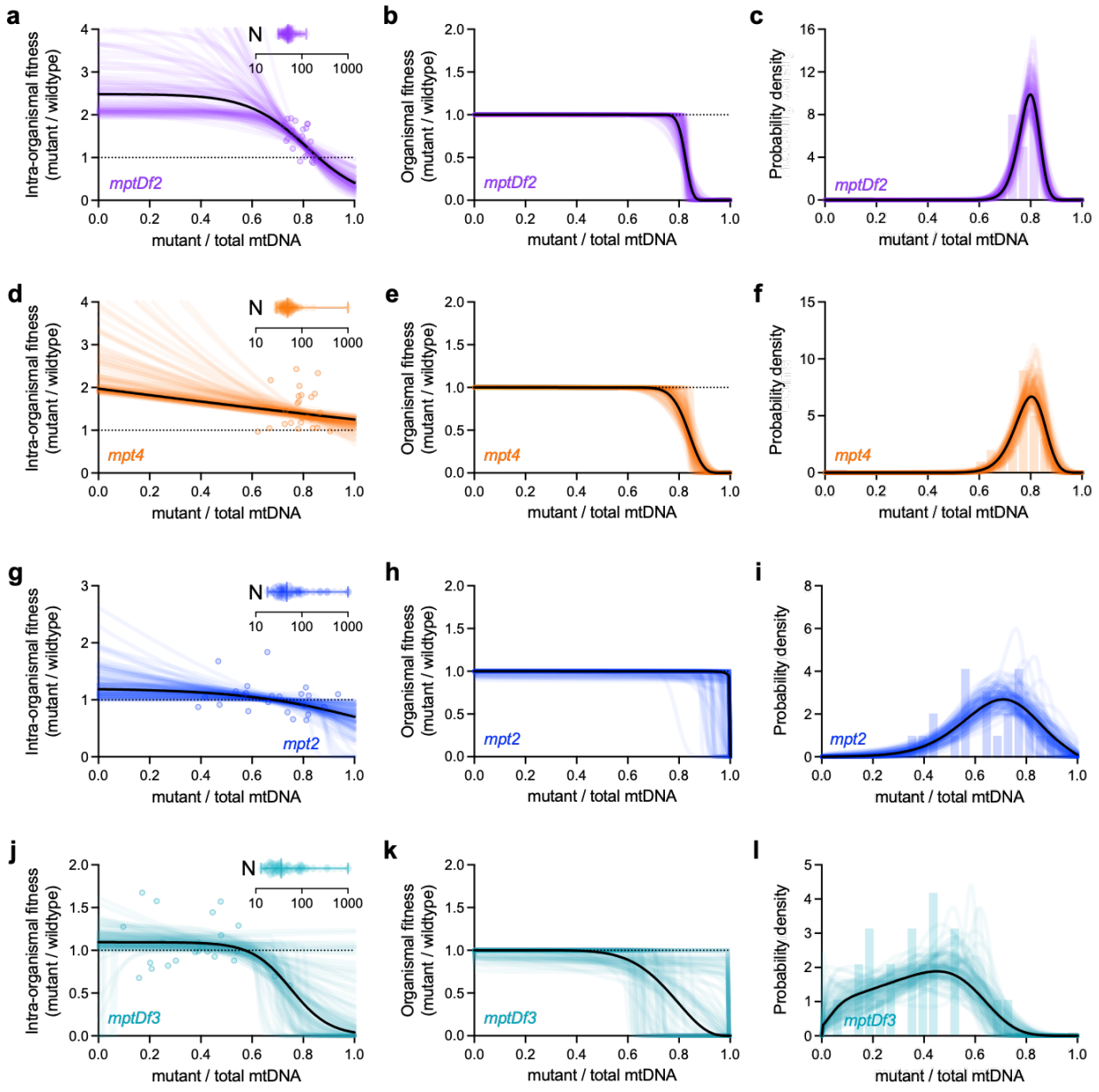

Figure 5: Integrating theoretical modeling with experiment shows the maintenance of selfish mitochondrial genomes in a heteroplasmic state through multiple distinct evolutionary mechanisms.

Maximum-likelihood estimates of intra-organismal (left column) and organismal (center column) fitness effects, each as a function of mutant frequency, together with the resulting most evolutionarily stable mutant frequency distribution (right column). Similar to bottom row of Fig. 3, but for the 4 mitochondrial genotypes shown in Fig. 4: *mptDf2* (**a-c**), *mpt4* (**d-f**), *mpt2* (**g-i**), and *mptDf3* (**j-l**). Each plot shows maximum-likelihood estimates corresponding to the empirical data represented in Fig. 4 (solid black line) and 100 parametric bootstrap data sets (colored lines) to visualize confidence estimates. Model parameters specifying intra-organismal selection, organismal selection, and intra-organismal drift (left column, insets, bars indicate mean, lowest and highest values), were collectively estimated using a joint maximum-likelihood approach that combines all 3 corresponding empirical data sets in Fig. 4.

Genotype	$w_{intra}(0)$	$w_{intra}(1)$	$z(w_{org}=0.5)$	Growth rate	N	Average z	SD z	Probability of loss
uaDf5	1.37 1.27–2.22	0.34 $5.8*10^{-4}$–1.12	0.77 0.75–0.82	0.77 0.75–0.80	29 20–100	0.63 0.59–0.65	0.13 0.10–0.15	$4.1*10^{-4}$ $3.7*10^{-6}$–$1.1*10^{-3}$
mptDf2	2.48 1.96–8.43	0.41 0.12–0.81	0.82 0.81–0.84	0.40 0.35–0.45	50 34–98	0.79 0.77–0.80	0.042 0.034–0.079	$3.6*10^{-18}$ $1.3*10^{-26}$–$7.0*10^{-6}$
mpt4	1.97 1.87–5.47	1.25 0.77–1.35	0.83 0.81–0.87	0.45 0.39–0.50	46 29–125	0.79 0.77–0.81	0.063 0.045–0.094	$1.4*10^{-9}$ $3.1*10^{-21}$–$9.3*10^{-6}$
mpt2	1.19 1.01–1.97	0.70 $4.8*10^{-5}$–0.98	>0.99 0.91–1	>0.99 0.92–1	44 24–1000	0.67 0.61–0.73	0.15 0.11–0.20	$9.9*10^{-5}$ $4.4*10^{-10}$–$2.2*10^{-3}$
mptDf3	1.10 0.89–1.40	0.04 0–1.09	0.77 0.63–1	0.93 0.83–1	23 15–707	0.38 0.30–0.45	0.18 0.15–0.20	0.02 $5.4*10^{-4}$–0.04

Table 1: Population genetic characteristics of five selfish mitochondrial genomes.

Each entry: maximum likelihood estimate (first line), 95% bootstrap confidence interval (second line).

w_{intra}: relative fitness of mutant genome (intra-organismal level)

w_{org}: relative fitness of mutant genome (organismal level)

N: per-generation effective mtDNA bottleneck size

z: average mutant mtDNA frequency among heteroplasmic hosts